Journal of Cerebral Blood Flow & Metabolism (2014) 34, 1148–1156

www.jcbfm.com

ORIGINAL ARTICLE

Radiosynthesis and validation of ^{18}F-FP-CMT, a phenyltropane with superior properties for imaging the dopamine transporter in living brain

Paul Cumming[1], Simone Maschauer[1], Patrick J Riss[2], Nuska Tschammer[3], Stefanie K Fehler[3], Markus R Heinrich[3], Torsten Kuwert[1] and Olaf Prante[1]

To date there is no validated, ^{18}F-labeled dopamine transporter (DAT) radiotracer with a rapid kinetic profile suitable for preclinical small-animal positron emission tomography (PET) studies in rodent models of human basal ganglia disease. Herein we report radiosynthesis and validation of the phenyltropane ^{18}F-FP-CMT. Dynamic PET recordings were obtained for ^{18}F-FP-CMT in six untreated rats, and six rats pretreated with the high-affinity DAT ligand GBR 12909; mean parametric maps of binding potential (BP_{ND}) relative to the cerebellum reference region, and maps of total distribution volume (V_T) relative to the metabolite-corrected arterial input were produced. ^{18}F-FP-CMT BP_{ND} maps showed peak values of $\sim$4 in the striatum, versus $\sim$0.4 in the vicinity of the substantia nigra. Successive truncation of the PET recordings indicated that stable BP_{ND} estimates could be obtained with recordings lasting only 45 minutes, reflecting rapid kinetics of ^{18}F-FP-CMT. Pretreatment with GBR 12909 reduced the striatal binding by 72% to 76%. High-performance liquid chromatography analysis revealed rapid metabolism of ^{18}F-FP-CMT to a single, non-brain penetrant hydrophilic metabolite. Total distribution of volume calculated relative to the metabolite-corrected arterial input was 4.4 mL/g in the cerebellum. The pharmacological selectivity of ^{18}F-FP-CMT, rapid kinetic profile, and lack of problematic metabolites constitute optimal properties for quantitation of DAT in rat, and may also predict applicability in human PET studies.

Journal of Cerebral Blood Flow & Metabolism (2014) **34,** 1148–1156; doi:10.1038/jcbfm.2014.63; published online 9 April 2014

Keywords: dopamine transporter; fluorine-18; phenyltropanes; positron emission tomography; rat

INTRODUCTION

The plasma membrane dopamine transporter (DAT) is abundantly expressed in the terminals of the nigrostriatal pathway and throughout the extended striatum, where it mediates the re-uptake of dopamine; the activity of DAT determines the spatial and temporal dynamics of dopamine signaling in the basal ganglia, and its expression is a sensitive indicator of the integrity of the nigrostriatal dopamine innervation. As such, DAT presents an important target for molecular imaging by positron emission tomography (PET) and single-photon computer tomography, in both research and clinical settings. We were interested in a DAT radiotracer to investigate the impact of nutrition and diabetes on dopaminergic signaling in rat models. However, because of constraints imposed by radionuclides other than ^{18}F in combination with the kinetic profiles of the available radiotracers in the required imaging protocols, there remains a need for a tracer with optimal properties for quantitative imaging of multiple animals from a single radiosynthesis. Although, a plethora of agents have been developed for imaging of DAT,[1–3] all may suffer in varying degrees from lack of selectivity, unfavorable kinetics, and adverse metabolism. A particular issue is the pharmacological selectivity of tracers for DAT versus serotonin transporters (SERT), and to a lesser extent (because of their low abundance) noradrenaline transporters (NET). Selectivity for DAT over SERT and NET is virtually absent for the prototypic DAT PET tracer ^{11}C-cocaine. Nonetheless, single-photon computer tomography ligands based upon the phenyltropane structure have found widespread use in clinical practice for the neurochemical diagnosis of Parkinson's disease; these include ^{123}I-β-CIT, ^{123}I-PE21,[4] and ^{123}I-FP-CIT (^{123}I-ioflupane, DATScan),[5,6] which has high striatal DAT binding, but some SERT binding in other brain regions.[7] These compounds are convenient for clinical procedures, as the radionuclides are suitable for distribution or local production, but the limited spatial resolution and imperfect quantitation of most single-photon computer tomography procedures does not afford detailed examination of striatal subregions. Furthermore, these compounds are generally characterized by slow kinetics, in some cases requiring many hours to obtain equilibrium, and in a number of instances their quantitation suffers from interference from SERT binding.

^{11}C-cocaine has rapid kinetics, but rather low specific binding in the human striatum,[8] and suffers from the lack of pharmacological selectivity noted above, although the preponderance of its striatal binding is with DAT.[9] In contrast, the active enantiomer of ^{11}C-methylphenidate has higher affinity and thus higher DAT

[1]Department of Nuclear Medicine, Laboratory of Molecular Imaging and Radiochemistry, Friedrich Alexander University, Erlangen, Germany; [2]Department of Chemistry, Universitetet i Oslo & Norsk Medisinisk Syklotronsenter AS, Oslo, Norway and [3]Department of Chemistry and Pharmacy, Pharmaceutical Chemistry, Emil Fischer Center, Friedrich Alexander University, Erlangen, Germany. Correspondence: Professor Dr O Prante, Department of Nuclear Medicine, Laboratory of Molecular Imaging and Radiochemistry, Friedrich Alexander University, Schwabachanlage 6, Erlangen 91054, Germany or Dr PJ Riss, Department of Chemistry, Universitetet i Oslo & Norsk Medisinisk Syklotronsenter AS, Postboks 1033- Blindern, 0315 Oslo, Norway.
E-mail: olaf.prante@uk-erlangen.de or Patrick.Riss@kjemi.uio.no
This study is part of the Neurotrition Project, which is supported by the Emerging Fields Initiative of the Friedrich-Alexander-Universität Erlangen-Nürnberg (FAU). RTI-121 was generously donated by Dr F Ivy Carroll (RTI International).
Received 28 November 2013; revised 19 February 2014; accepted 16 March 2014; published online 9 April 2014

binding in the striatum, but also reveals specific binding to NET in the thalamus and cortex,[10] consistent with its near equipotency at inhibiting the two transporters.[11] Quantitation of the selective DAT ligand ^{11}C-PE2I may be confounded by the formation of a brain-penetrating metabolite.[12] In general, logistic limitations arise from the short physical half-life of carbon-11, which does not afford multiple scanning sessions from a single radiosynthesis. In this respect, the 110 minutes half-life of fluorine-18 can present distinct advantages; however, neither cocaine, nor methylphenidate offers a possibility for ^{18}F-labeling. Most of the validated ^{18}F-labeled candidates for DAT imaging have low *in vivo* stability and slow attainment of equilibrium binding. A tremendous effort has been expended in the search for an optimal DAT radiotracer; this effort has led to an exemplary understanding of the challenges in the field of DAT imaging, especially as pertains to the phenyltropane lead structure.[2,13–15] ^{18}F-FP-CIT, arguably the best of the ligands for human studies, attained very high peak binding in the human striatum during the interval of 60 to 90 minutes post injection;[16] its kinetics in rodent have not been reported, but structurally identical ^{123}I-FP-CIT peaks at 1 hour in the rat striatum.[7] Whereas ^{18}F-FE-CNT has good selectivity for DAT and rapid kinetic profile in humans, a polar metabolite resulting from oxidative cleavage of the N-substituent may confound its utility in the rat.[15,17,18] ^{18}F-CFT (^{18}F-WIN 35,428) attained even higher binding than ^{18}F-FE-CNT in the human striatum, peaking 4 hours after tracer injection;[19] rodent studies *ex vivo* revealed some binding to NET in the extrastriatal regions,[20] but the main limitation of these tracers is their requirement for long scans.

An ideal ligand for PET studies of DAT would contain fluorine-18, and attain equilibrium binding within less than 1 hour, giving abundant signal in the striatum with high selectivity for DAT over other monoamine transporters, and would not yield a brain-penetrating metabolite, which facilitates quantitative PET imaging studies using the reference tissue model. No validated radiotracer perfectly meets the optimal requirement for PET imaging in rat, which is a major impediment for the use of PET in rat models of basal ganglia disease. General findings of phenyltropane chemistry have indicated that the N-substituent should be longer than two carbons so as to minimize oxidative dealkylation *in vivo*, which would otherwise yield a brain-penetrating metabolite. In addition, the 4-position of the phenyl ring should carry a substituent no larger than a methyl group to retain high DAT selectivity. In the course of a concerted search for such a compound in the literature, we noted the properties of FP-CMT, an N-fluoropropyl phenyltropane with 30-fold selectivity for DAT over SERT and NET from rat brain,[20] and which had been labeled with fluorine-18.[21] However, its suitability as a PET ligand had not been further investigated. In the present study, we established an improved radiosynthesis of ^{18}F-FP-CMT and undertook a series of rat PET examinations; we calculated parametric maps of the binding potential (BP_{ND}) relative to a reference region and the total distribution volume (V_T; mL/g) relative to a metabolite-corrected arterial input in groups of untreated anaesthetized rats, and in rats pretreated with the DAT-specific ligand GBR 12909. We also measured saturation-binding parameters of ^{18}F-FP-CMT in the rat striatum, and verified the selectivity of FP-CMT for hDAT using an uptake assay *in vitro*, thus supporting the potential of this tracer for translational imaging in humans.

MATERIALS AND METHODS

General

The details on (radio)chemistry methods are described in the Supplementary Data. All animal experiments were performed in compliance with the guidelines and recommendations on laboratory animal science disciplines by the Federation of European Laboratory Animal Science Associations (FELASA) using the protocols approved by the local Animal Protection Authorities (Regierung Mittelfranken, Ansbach, Germany, No. 54-2532.2-18/12).

In Vitro Uptake Inhibition Assays

The hDAT plasmid was a generous gift of Patrick Schloss (Central Institute of Mental Health, Mannheim, Germany). hSERT pcDNA3 (plasmid #15483) and hNET pcDNA3 (plasmid #15475) were purchased from AddGene (www.addgene.org). CHO-K1 cells (ATCC) were grown in DMEM/F-12 supplemented with 10% fetal bovine serum, 2 mmol/L *L*-glutamine, 1% penicillin-streptomycin (all from Life Technologies, Darmstadt, Germany) and maintained at 37°C in 5% CO_2. Upon confluency, 50% to 70% of the cells were transfected with hDAT, hSERT, or hNET using the Mirus2020 (Mirus Bio LCC, Madison, WI, USA) transfection reagent according to the manufacturer's instructions. The next day, cells were seeded in 96-well plates (Greiner Bio-One GmbH, Frickenhausen, Germany) at a density of 40,000 cells per well and left overnight to adhere. On the day of experiment, the medium was removed, and the test compounds (FP-CMT (see Supplementary Data) or cocaine were added in a range of final concentrations in Hank's Balanced Salt Solution. After incubation for 30 minutes at 37°C, the fluorescent dye (neurotransmitter transporter uptake assay, Molecular Devices, Biberach, Germany) was added to the medium; uptake after 60 minutes was recorded with a Victor^{3}V microplate reader in fluorescence mode (excitation 430 nm, emission: 510 nm, bottom reading). No increase in fluorescence was indicative of complete inhibition of the respective transporter. The uptake data were analyzed using algorithms in PRISM 5.0 (GraphPad software, San Diego, CA, USA) using a single site model. The dose-response curves of 2 to 4 experiments were performed in triplicate, normalized to maximal uptake, and pooled to produce a mean sigmoidal curve from which the IC_{50} value and maximum intrinsic blocking for each compound was obtained.

Receptor Autoradiography *In Vitro*

Rats from four control PET studies were killed by decapitation while anesthetized. Brains were quickly removed and frozen by immersion in isopentane cooled to -40°C by addition of granular dry ice. Horizontal brain sections (20 μm) passing through the mid striatum and cerebellum were cut on a cryostat microtome (HM550, Microm, Waldorff, Germany), thaw-mounted pairwise on glass slides (Histobond, Marienfeld GmbH, Lauda Königshofen, Germany) and stored at -20°C. DAT binding was measured using ^{125}I-RTI-121 (81.4 TBq/mmol, PerkinElmer, Boston, MA, USA) after a procedure described by Quik *et al*[22] In brief, thawed sections were dried at room temperature and preincubated for 15 minutes at room temperature in 50 mmol/L Tris-HCl, 120 mmol/L NaCl, and 5 mmol/L KCl, 1 μmol/L fluoxetine (Biotrend, Switzerland), pH 7.4 (buffer A). After removal of buffer, slides were transferred to chambers containing buffer A modified by addition of 11 pM ^{125}I-RTI-121 and eight different concentrations of non-radioactive RTI-121 (0.1 to 200 nmol/L) (generous gift of Dr F Ivy Carroll, RTI International, Research Triangle Park, USA). Slide-mounted sections were washed (3×15 minutes) in buffer A at 4°C, dipped in ice-cold water, and dried under a stream of cool air, and exposed for 2 to 4 days to a phosphor screen (BAS-IP SR 2040, GE Healthcare Europe GmbH, Freiburg, Germany) together with an iodine-125 standard strip (ARC, American Radiolabeled Chemicals, St Louis, MO, USA).

Saturation-binding experiments with ^{18}F-FP-CMT were performed similarly as for ^{125}I-RTI-121, except that the incubation buffer was modified by the addition of eight different ^{18}F-FP-CMT concentrations (1.5 to 300 nmol/L). After incubation for 1 hour, slides were washed (2×60 seconds) in ice-cold buffer A, dipped in ice-cold water, dried, and placed overnight on a phosphor screen. One slide carried the dried residues of 5 μL of each incubation solution, to serve as fluorine-18 standards; here the signal intensity for each spot was corrected for the surface area defined by thresholding, and for 20 micron tissue thickness, assuming brain density of 1 g/mL, and assuming zero tissue attenuation of the positron ($E_{max} = 635$ keV). Exposed screens were analyzed with a high-resolution radioluminography laser scanner (DÜRR Medical HD-CR 35 Bio, Raytest, Straubenhardt, Germany) using the software AIDA Image Analyzer to quantitate radioligand binding. The optical density values were converted to pmol per gram of tissue relative to the standards. Specific binding in a large circular region of interest placed in the striatum (four striata per slide) was determined by subtracting corresponding cerebellum values, which were linear with ligand concentration. The saturation-binding parameters B_{max} and K_d were calculated for ^{125}I-RTI-121 and ^{18}F-FP-CMT using the software GraphPad Prism (version 5.0, GraphPad Software, La Jolla, USA), assuming a one-site model.

Positron Emission Tomography Studies

Female Sprague–Dawley rats (Charles River) weighing 240 to 280 g and 10 to 14 weeks old were used for this study, which was approved by the local

Animal Protection Authorities (Regierung Mittelfranken, Germany, 54-2532.2-18/12). Small-animal PET imaging studies were conducted on the Inveon microPET scanner (Siemens Healthcare, Erlangen, Germany). After intravenous injection of ^{18}F-FP-CMT (8–15 MBq), dynamic emission recordings consisting of 24 frames of duration increasing from 30 seconds to 15 minutes were acquired to a total of 60 minutes (2 hours in the pilot studies), followed by an attenuation scan using a rotating ^{57}Co point source. Dynamic emission images were corrected for attenuation and decay, and reconstructed by the iterative maximum a posteriori estimation, using software installed in the Inveon PET for dead time and random correction. The dynamic PET scan was converted to MINC format (McConnell Brain Imaging Centre, Montreal Neurological Institute), and summation images were calculated and co-registered with an anatomic template of the rat brain using a seven parameter rigid body transformation (for details see Supplementary Data). This transformation was then used to resample the dynamic recording in MINC format to the standard coordinates for rat brain, and templates for the entire cerebellum and for the bilateral striatum were applied to extract time-activity curves for the two tissues. Preliminary analysis (see Supplementary Data) showed no significant time dependence of the distribution volume ratio between 60 and 120 minutes (data not shown); subsequent emission recordings were confined to 60-minute duration.

For the quantitative studies, rats were implanted with catheters (Portex Fine Bore polyethylene tubing, 0.4 mm ID, 0.8 mm OD, Smiths Medical, Grasbrunn, Germany) to the left femoral vein and artery while anesthetized with isoflurane (2% in oxygen). The wound was sutured, and the animals transferred to the tomograph, and maintained under isoflurane anesthesia; one group of ($n = 6$) TOTAL rats received no pretreatment, whereas another group of ($n = 6$) BLOCKED rats were pretreated with GBR 12,909 (12.5 mg/kg, intraperitoneal, Tocris Bioscience, Bristol, UK) at 15 minutes before tracer injection A first arterial blood sample (250 μL) was collected at 1 minute after tracer injection to the femoral vein, and subsequent samples (100 μL) collected at 2, 5, 10, 15, 30, 45, and 60 minutes, in the course of a dynamic emission recording.

The blood samples were centrifuged and the total radioactivity concentration in 10 μL portions of plasma were measured with a gamma counter (Wallac Wizard, PerkinElmer) and decay-corrected in units of Bq/mL to the time of tracer injection. Remaining portions of plasma were deproteinated by the addition of 10% aqueous TFA, centrifuged, and the supernatants analyzed by reversed phase high-performance liquid chromatography. The analytical system consisted of a Luna C18 (2) column measuring 150 × 4.6 mm, with mobile phases as above except in 25:75 proportions of the component solutions, delivered isocratically at a flow rate of 1.5 mL/minute. Fractions were collected at intervals of 1 minute and ^{18}F-activity measured in the gamma counter. Under these conditions, the retention factor k′ ($k' = (t_R - t_0)/t_0$); t_R: retention time; t_0: column dead- time) of the parent compound was 6.2 and that of the single hydrophilic radio metabolite was 0.36. Proportions of untransformed tracer and a single hydrophilic metabolite were calculated at each measured time point, and the total arterial input curve was corrected for metabolism as described previously.[23] Using the plasma time-activity curves calculated from the untransformed ^{18}F-FP-CMT and its single hydrophilic metabolite, the fractional rate constants for whole body tracer metabolism (k_0; 1/minute) and for elimination from plasma of the metabolite (k_{-1}; 1/minute) were calculated by linear regression analysis as described previously.[24] From the initial 1-minute blood sample, a 50 μL portion of plasma was transferred to a Roti-Spin tube (MWCO = 10 kDa, Carl Roth, Karlsruhe, Germany), and then centrifuged at 10,000 *g*; the radioactivity in a 20 μL portion of the ultrafiltrate was measured in the gamma counter, and the free fraction was calculated relative to the total radioactivity in the entire plasma sample.

In the main study of untreated (TOTAL) and GBR 12909-treated (BLOCKED) rats, the BP_{ND} in the striatum volume of interest was calculated by the Lammertsma Simplified Reference Tissue Method[25] and by the Logan reference tissue method (as distribution volume ratio-1)[26] using the entire 60-minute recordings, and with truncation to 50, 40, and 30 minutes, and always with exclusion of the first 7 minutes from the Logan linearization. The total distribution volumes (V_T; mL/g) in the cerebellum and striatum volume of interests were calculated for 60-minute recordings relative to the metabolite-corrected arterial inputs, and also with correction to the individual free fraction of ^{18}F-FP-CMT in plasma (V_T/fp). Individual parametric maps of BP_{ND} relative to the cerebellum reference tissue were calculated by the Zhou Simplified Reference Tissue Method[27] using the entire 60-minute recordings, and corresponding parametric maps of V_T and V_T/fp were calculated by the Logan arterial input method[28] using the

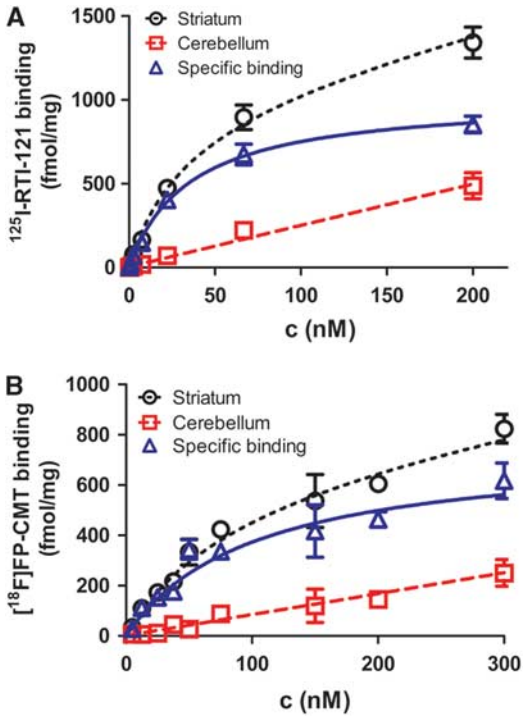

Figure 2. Mean plots of four independent saturation-binding assays for (**A**) ^{125}I-RTI-121 and (**B**) ^{18}F-FP-CMT. Values are mean ± s.d. Non-specific binding measured in the cerebellum was linear with concentration for both ligands. Total binding in the striatum, after subtraction of non-specific binding, reveals the specific binding curve for the two ligands, to which is fitted a one-site model yielding the saturation-binding parameters B_{max} and K_d.

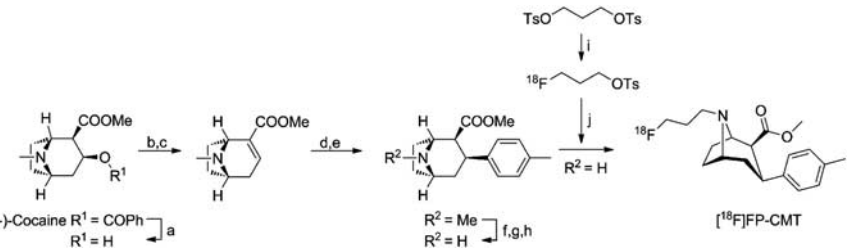

Figure 1. Synthesis of ^{18}F-FP-CMT. a: 0.8 M HCl, reflux, 16 hours;[42] b: $POCl_3$, reflux, 1 hour; c: MeOH, −78°C to room temperature (RT);[43] d: MePhMgBr, Et_2O, CH_2Cl_2, −78°C, 2 hours, −43°C, 3 hours; e: TFA/CH_2Cl_2, −78°C, 30 minutes;[43] f: $ClCO_2CHClCH_3$, $C_2H_4Cl_2$, reflux, 1 hour;[43] g: DIPEA, reflux, 1 hour;[43] h: MeOH (anhydrous), reflux, 2 hours;[43] i: [$K^+ \subset 222$]$^{18}F^-$, MeCN, 85°C, 2 minutes; j: nor-β-CMT, DMF, 130°C, 20 minutes.

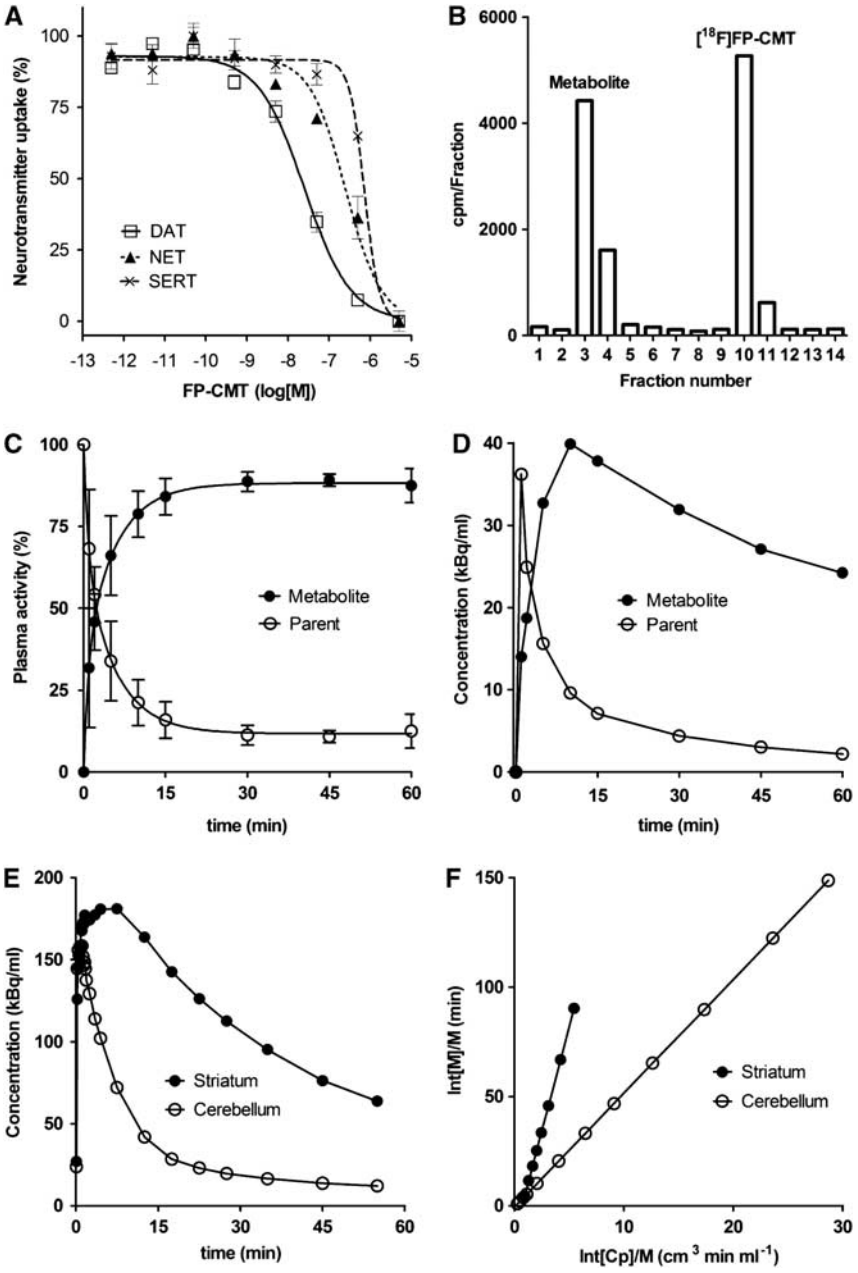

Figure 3. (**A**) Competitive uptake assays over a range of concentration of FP-CMT against human dopamine transporter (DAT), noradrenaline transporters (NET), and serotonin transporters (SERT) expressed in cell culture; curves are the fitting of the EC_{50}s to the observed data. Values are mean ± s.e.m. (**B**) Representative radiochromatogram of a plasma extract at 5 minutes after intravenous administration of ^{18}F-FP-CMT, (**C**) the mean fractions of parent and metabolite as a function of ^{18}F-FP-CMT circulation time in six control rats, values are mean ± s.d., and (**D**) the corresponding time-activity curves for parent and metabolite of a representative rat. (**E**) Time-activity curves measured in the cerebellum and striatum of a representative untreated rat, and (**F**) Logan plots of the corresponding brain recordings relative to the arterial input function.

program Pip (Ole L. Munk, Aarhus PET Centre). The resultant parametric maps were transformed to MINC format, resampled to standard coordinates, and mean maps for the TOTAL and BLOCKED groups were calculated.

RESULTS

The radiosynthesis of ^{18}F-FP-CMT was performed after the procedure by Chaly *et al*,[21] with some modifications. By careful verification of the one-pot radiosynthesis in our laboratory, we established an improved experimental procedure with optimized reaction time (50 minutes), improved decay–uncorrected radiochemical yield (15%) and high specific activity of ^{18}F-FP-CMT (Figure 1, see Supplementary Data File). This radiosynthesis yielded sufficient amounts of ^{18}F-FP-CMT in a reliable manner to proceed with extended *in vitro* and *in vivo* studies.

Mean plots of four independent saturation-binding assays for ^{125}I-RTI-121 (Figure 2A) and ^{18}F-FP-CMT (Figure 2B) are consistent with a single binding site in the rat striatum, with B_{max} 1021 ± 89 pmol/g and K_d 34 ± 12 nmol/L for ^{125}I-RTI-121 and B_{max} 730 ± 152 pmol/g and K_d 91 ± 24 nmol/L for ^{18}F-FP-CMT ($P < 0.02$ for both parameters). The uptake inhibition curves for FP-CMT

Table 1. The BP_{ND} of ^{18}F-FP-CMT in the striatum[a]

	Lammmertsa simplified reference tissue				*Logan reference tissue*			
	60 minutes	*50 minutes*	*40 minutes*	*30 minutes*	*60 minutes*	*50 minutes*	*40 minutes*	*30 minutes*
TOTAL ($n=6$)	2.69 ± 0.31	2.60 ± 0.30	2.61 ± 0.30	2.53 ± 0.29	2.50 ± 0.25	2.33 ± 0.21	2.16 ± 0.24	1.90 ± 0.14
BLOCKED ($n=6$)	0.74 ± 0.32 (− 72%)	0.75 ± 0.32 (− 72%)	0.77 ± 0.32 (− 71%)	0.79 ± 0.35 (− 71%)	0.65 ± 0.28 (− 76%)	0.68 ± 0.29 (− 75%)	0.72 ± 0.31 (− 73%)	0.74 ± 0.32 (− 72%)

BP, binding potential. [a]Values are expressed as mean ± s.d. for groups of untreated (TOTAL) and GBR 12909-treated (12.5 mg/kg, intraperitoneally, BLOCKED) rats calculated relative to the cerebellum reference tissue, with progressive truncation of scan duration from 60 minutes to 30 minutes.

Table 2. The distribution volume (V_T) of ^{18}F-FP-CMT in striatum and cerebellum[a]

	Striatum V_T (mL/g)	*Cerebellum V_T (mL/g)*	*BP_{ND} (DVR-1)*	*Plasma-free fraction*	*Striatum V_T/fp (mL/g)*	*Cerebellum V_T/f_p (mL/g)*
TOTAL ($n=6$)	15.5 ± 3.8	4.45 ± 0.80	2.47 ± 0.41	0.14 ± 0.05	134 ± 61	39 ± 16
BLOCKED ($n=6$)	12.8 ± 1.2	7.15 ± 1.15 (+ 61%)	0.76 ± 0.37 (− 69%)	0.19 ± 0.12	78 ± 41	51 ± 33
P	NS	0.012	< 0.001	NS	NS	NS

BP_{ND}, binding potential; DVR, distribution volume ratio ; NS, not significant; V_T , total distribution volume. [a]Values are expressed as mean ± s.d. in groups of untreated (TOTAL) and GBR 12909-treated (12.5 mg/kg, intraperitoneally, BLOCKED) rats calculated by the Logan linearization relative to the metabolite-corrected arterial input function measured during 60 minutes, along with the resultant estimates of binding potential (BP_{ND}). Also presented are the mean estimates of the ^{18}F-FP-CMT plasma-free fraction (f_p), and the distribution volumes (V_T) corrected for the individual free fraction. *P* is the significance of group difference between TOTAL and BLOCKED results by the 2-tailed *t*-test.

against the three human transporters are illustrated in Figure 3A. FP-CMT inhibited hDAT with $IC_{50} = 27.5$ nmol/L ($pIC_{50} = 7.56 \pm 0.07$), hNET with $IC_{50} = 307$ nmol/L ($pIC_{50} = 6.51 \pm 0.15$), and hSERT with $IC_{50} = 1708$ nmol/L ($pIC_{50} = 5.77 \pm 0.12$). Under the same conditions cocaine (not illustrated) inhibited hDAT with $IC_{50} = 380$ nmol/L (pIC_{50} 6.42 ± 0.14), hNET with $IC_{50} = 3800$ nmol/L (pIC_{50} 5.42 ± 0.19), and hSERT with $IC_{50} = 1400$ nmol/L (pIC_{50} 5.86 ± 0.20). The overall mean of the octanol/water partition coefficient for ^{18}F-FP-CMT was $logD_{7.4} = 1.04 \pm 0.02$.

The *in vitro* incubation showed complete stability of ^{18}F-FP-CMT for up to an hour in human plasma and serum (data not shown). High-performance liquid chromatography analysis of plasma extracts from arterial blood collected during the rat PET recordings revealed the presence of a single hydrophilic-labeled metabolite (Figure 3B). Time courses of the parent compound and metabolite fractions (Figure 3C) and concentrations (Figure 3D) during 60 minutes showed rapid metabolism in living rat, and relative retention of the metabolite in the plasma compartment. The kinetic analysis of plasma tracer kinetics (not illustrated) revealed a fractional rate constant for the metabolism of ^{18}F-FP-CMT (k_0) of 0.31 ± 0.10 min^{-1} in ($n=6$) untreated rats and 0.29 ± 0.13 min^{-1} in ($n=6$) GBR 12909-treated rats; the corresponding fractional rate constants for clearance of the single hydrophilic metabolite from plasma (k_{-1}) were 0.054 ± 0.014 min^{-1} and 0.040 ± 0.043 min^{-1}. The mean plasma-free fractions measured at one minute after injection were 14 ± 5% for untreated rats and 19 ± 12% (+ 35%) for GBR 12909-treated rats ($P = 0.44$).

Time-activity curves measured in cerebellum showed rapid washout, whereas there was considerable retention of radioactivity in the striatum (Figure 3E). The volume of interest analysis by the Lammertsma Simplified Reference Tissue Method showed a mean BP_{ND} in striatum of 2.69 ± 0.31, which declined by 6% with truncation of scan duration from 60 minutes to 30 minutes (Table 1); in contrast, mean BP_{ND} by the Logan reference tissue method[29] declined from 2.50 ± 0.25 by 24% with this truncation. In the blocking studies, striatal BP_{ND} was reduced by 71% to 76%, depending on the method and scan truncation; the difference between TOTAL and BLOCKED groups was always highly significant ($P < 0.001$). Representative arterial input Logan plots for cerebellum and striatum in a TOTAL rat are illustrated in Figure 3F. The mean magnitude of V_T relative to the metabolite-corrected arterial curve in the cerebellum increased from 4.45 ± 0.08 mL/g in the TOTAL condition by 61% ($P = 0.012$) in the BLOCKED condition (Table 2), but GBR 12909 treatment was without significant effect on V_T in the striatum.

Mean parametric maps of BP_{ND} show specific binding nearly restricted to the striatum of the untreated rats group (Figure 4A), with substantial declines in striatal binding of the BLOCKED rats (Figure 4B). We see a homogeneous non-displaceable background BP_{ND} of ~0.4 throughout the telencephalon; considering this to be an artefact of the reference tissue method (see Discussion), and subtracting this apparent binding from the striatum measurements increased the apparent blockade by GBR 12909 treatment from 72% to 85% in striatum. There was some specific binding in the ventral midbrain (Figure 4C), which we attribute to the substantia nigra, with displaceable BP_{ND} of ~0.4. Mean parametric maps of V_T in the TOTAL (Figure 5A) and BLOCKED (Figure 5B) groups are consistent with the BP_{ND} maps, and reveal the globally increased V_T in non-binding regions (notably the cerebellum) with GBR 12909 treatment. Voxel-wise correction of V_T for the plasma-free fraction of ^{18}F-FP-CMT shows substantial global scaling, and a suggestion of relatively lesser group difference in V_T/f_p for cerebellum of the TOTAL and BLOCKED groups (Figure 5C). Table 2 shows that correcting V_T for the plasma-free fraction resulted in considerably less precision of the estimates of V_T/f_p.

DISCUSSION

We report the results of a series of experiments *in vitro* and *in vivo* designed to assess the phenyltropane ^{18}F-FP-CMT for quantitation of DAT in living brain. With respect to binding at transporters *in vitro*, our compound exhibited 10-fold selectivity for hDAT over hNET, and 60-fold selectivity over hSERT. These findings are roughly in accordance with earlier results from rat brain

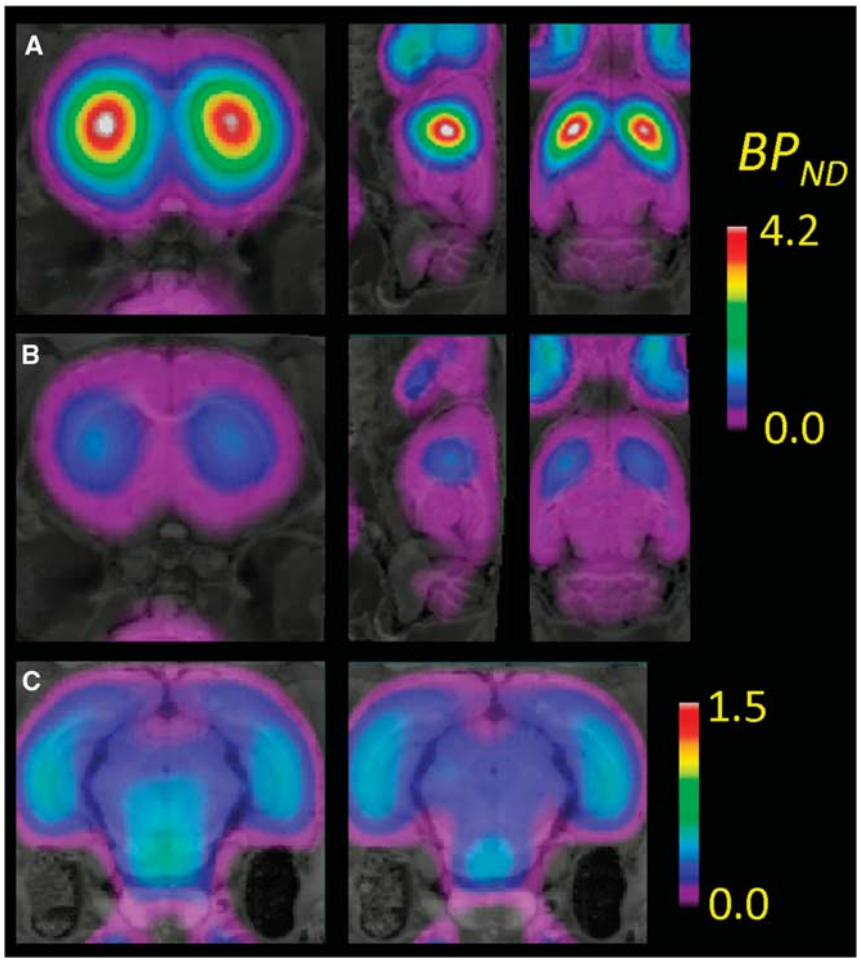

Figure 4. Mean parametric maps of six separate determinations of ^{18}F-FP-CMT BP_{ND} in the three planes, projected onto the rat brain anatomic atlas for (**A**) TOTAL, i.e., the untreated rat group, and (**B**) BLOCKED, the rats pretreated with GBR 12909 (12.5 mg/kg, intrapertioneally), along with (**C**) corresponding findings in the vicinity of the substantia nigra.

homogenates[20] albeit with lower selectivity for the hNET, but predict that ^{18}F-FP-CMT may also serve for selective DAT imaging in human brain. The IC_{50} of ^{18}F-FP-CMT about hDAT was 10-fold higher than that of cocaine, consistent with the high binding of ^{18}F-FP-CMT seen in PET studies. Autoradiographic saturation-binding studies of DAT in rat brain sections indicated a lower affinity of ^{18}F-FP-CMT (91 nmol/L) relative to that of ^{125}I-RTI-121 (34 nmol/L); this difference may account for the PET tracer's rapid kinetics *in vivo*, as discussed below. The B_{max} *of* ^{18}F-FP-CMT in the rat striatum was significantly less than that of ^{125}I-RTI-121, but was more variable, perhaps because of the lower affinity, which we suspect results in greater loss of specific binding during the brief washing step. Our autoradiographic B_{max} in the rat striatum matches closely with the findings of ^{3}H-WIN 35,428 in the tree shrew (700 pmol/g);[28] we have been unable to find comparable measurements in rat. Positron emission tomography findings of DAT B_{max} for ^{11}C-cocaine in human striatum (600 pmol/g),[8] exceed corresponding PET estimates in the rat striatum for ^{11}C-methylphenidate (400 pmol/g)[30] and ^{11}C-CFT (190 pmol/g);[31] since PET-derived measurements in rat are likely degraded by effects of partial volume, we conclude that DAT B_{max} in the mammalian striatum is similar *in vivo* and *in vitro*. This is in contrast to findings for dopamine $D_{2/3}$ receptors, which are seemingly fivefold more abundant in autoradiograms than in living brain, presumably reflecting compartmentation.[32]

The radioligand ^{18}F-FP-CMT proves to have a rather low octanol distribution coefficient in comparison with many successful PET tracers, but is close to that reported for ^{11}C-flumazenil and *N*-^{11}C-methylspiperone, both of which have high penetration of the blood–brain barrier.[33] In any event, the dynamic time-activity curves show rapid and substantial uptake of ^{18}F-FP-CMT in the striatum and cerebellum. We were unable to calculate the unidirectional blood–brain clearance (K_1; mL/g per minute) of our radioligand because of undersampling of the arterial input curve, but it is clear from brain uptake that ^{18}F-FP-CMT in arterial blood is efficiently extracted to brain; kinetic analysis of ^{18}F-FP-CIT uptake in human brain revealed an extraction fraction of 0.6.[16]

The kinetic analysis of plasma metabolism revealed rather rapid decomposition (k_0; 1/minute) of ^{18}F-FP-CMT, at $\sim$30% per minute. However, the rate constant for elimination of the single metabolite detected in plasma extracts ($k_{_1}$; 1/minute) was relatively slow, at $\sim$5% per minute. Plasma tracer kinetics was unaltered in rats with GBR 12909 pretreatment. Given its rapid metabolism, the ^{18}F-FP-CMT concentration in plasma has a rather narrow peak after bolus injection, and is rapidly surpassed in concentration by the labeled metabolite because of its slow elimination kinetics. The retention time of this metabolite by high-performance liquid chromatography indicates that it is very hydrophilic, presumably a 4-carboxy-analogue of ^{18}F-FP-CMT, and therefore highly unlikely to contribute to brain radioactivity during the PET recording. The

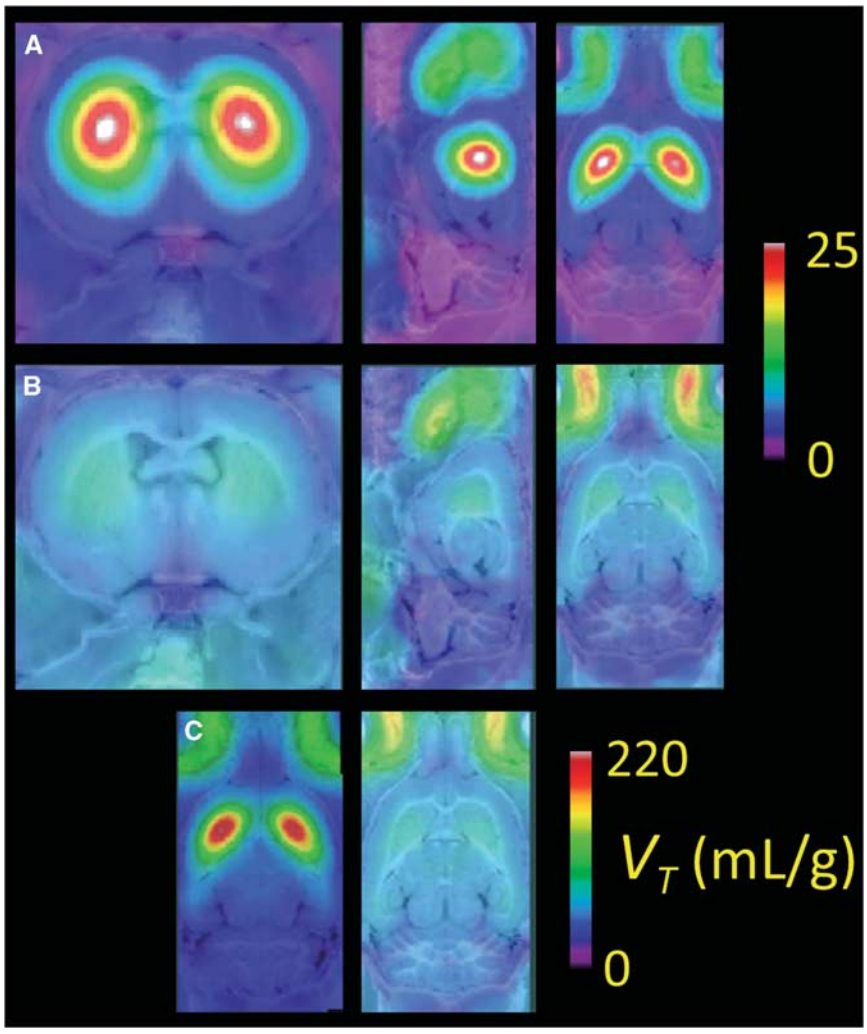

Figure 5. Mean parametric maps of six separate determinations of the ^{18}F-FP-CMT distribution volume (V_T) in the three planes projected on the rat brain anatomic atlas for (**A**) TOTAL, that is, the untreated rat group, and (**B**) BLOCKED, that is, that rats were pretreated with GBR 12909 (12.5 mg/kg), along with (**C**) a depiction of the corresponding mean V_T maps with correction for the plasma-free fraction of ^{18}F-FP-CMT.

complete lack of bone uptake of ^{18}F-fluoride (Figure 4) suggests that ^{18}F-FP-CMT is not dealkylated and then defluorinated by hepatic CYP enzymes, in contrast to the 4-fluorobut-2-enyl phenyltropane ^{18}F-LBT-999.[13]

The washout of ^{18}F-FP-CMT from rat cerebellum is rapid; qualitatively, the time course resembles that of ^{11}C-cocaine in human brain, being substantially complete in an hour;[8,9] the magnitude of ^{18}F-FP-CMT V_T in the cerebellum is also similar to that reported for ^{11}C-cocaine. We expected the magnitude of V_T to be unaffected by treatment with a DAT blocking agent, i.e., indicating lack of displaceable binding in the reference tissue. However, we noted a significant 61% increase in the cerebellum V_T in rats pretreated with GBR 12909; this increase is clearly evident in the parametric maps (Figure 5). In general, this phenomenon suggests increased bioavailability due to the blockade of peripheral binding sites for the ligand. While DAT is present in a number of peripheral tissues, we note that the ^{18}F-FP-CMT f_p of only (14%) is consistent with substantial binding to serum albumin. The free fraction tended to increase in the GBR 12909 group, driven by very high f_p measurements (30%) in three of six animals; the non-significant 35% increase in free fraction seems likely to be a driver for the 61% increase in the cerebellum V_T in the blocked condition, but the precision of the present estimates is insufficient to make strong claims in this regard. Correcting V_T for individual f_p suggested a rather high partitioning between brain ^{18}F-FP-CMT and the free ligand in plasma (circa 40 mL/g; Table 2).

In the absence of any evidence to the contrary, we consider the cerebellum to be a fit reference tissue for quantitation of ^{18}F-FP-CMT BP_{ND} in the rat telencephalon. Indeed, literature reports indicate that the density of DAT in the rodent striatum is only 0.4 pmol/g,[34] less than 0.1% of the striatal concentration. As such, traces of specific binding in the reference region can be safely ignored. The magnitude of the BP_{ND} in striatum, almost three, exceeds that reported for ^{11}C-methylphenidate by more than two-fold.[30] ^{18}F-CFT attained a binding ratio in rat striatum as high as 10, but this peak occurred more than 1 hour after tracer injection, which would require more extended recordings for quantitation.[19] Some new *N*-fluoropyridyl-containing tropanes with high selectivity for DAT also attained binding ratios as high as three in the rat striatum *ex vivo* after several hours,[35] and the phenyltropane ^{18}F-MCL-322 was likewise characterized by a ratio of barely three after several hours, because of very slow washout of the bound tracer.[36] In general, high-affinity candidates for DAT imaging show higher binding ratios,[14,37] but the attainment of equilibrium can then be substantially delayed. In contrast, ^{18}F-FP-CMT attains peak binding in the striatum within minutes, and has rapid washout, with kinetics comparable with those of ^{11}C-cocaine, but with

considerably higher BP_{ND}, reflecting its 10-fold higher affinity for DAT. Our systematic examination of effects of truncating the PET recording indicated that striatal BP_{ND} was quantifiable in the rat striatum with dynamic recordings as brief as 30 minutes with only a small underestimation relative to 1-hour recordings; we now routinely obtain 45-minute dynamic recordings, and have completed as many as four successive PET recordings from a single ^{18}F-FP-CMT radiosynthesis.

^{11}C-methylphenidate and ^{18}F-CFT, among other DAT tracers, might be expected to convey some signal arising from NET in the extrastriatal regions. However, even in the thalamus and midbrain, where NET is most abundant, a selective and high-affinity NET ligand had a BP_{ND} of only 0.5.[38] In the present context, interference from NET binding is rather a moot point, as we find 10-fold selectivity of ^{18}F-FP-CMT for hDAT over hNET, and even greater selectivity over hSERT, roughly as reported in the initial report of FP-CMT against the transporters in rat brain.[20] Examination of the parametric maps does not reveal any excess binding in the thalamus, or indeed anywhere in the brain, with the exception of a small displaceable DAT binding component near the substantia nigra; this mesencephalic binding represent a BP_{ND} close to 0.4, that is, 15% of the specific binding in striatum, which is in close agreement with the autoradiographic findings in mice.[39] The same parametric maps suggest a homogeneous non-displaceable background of BP_{ND} close to 0.4 throughout the forebrain. We believe this to arise from our use of a reference tissue template encompassing the entire rat cerebellum, from which the signal is likely to be decreased because of the spill-over of radioactivity at the edges of the structure. We used the entire cerebellum rather than a smaller central portion so as to optimize precision of the BP_{ND} measurement, presumably with some penalty in accuracy. The non-displaceable global background BP_{ND} (0.4), which we have also seen in rat studies of dopamine $D_{2/3}$ receptors with ^{11}C-raclopride,[40] may account for one half of the residual striatal BP_{ND} in the condition of GBR 12909 blocking. Thus, by this argument, the 72% blockade in the striatum may be underestimated, with true blocking as high as 85%. Similar findings have been reported in blocking studies with the DAT ligand ^{11}C-PR04.MZ.[41]

In summary, we implemented the radiosynthesis of ^{18}F-FP-CMT as a one-pot procedure that is highly amenable for automation, providing ^{18}F-FP-CMT for preclinical imaging studies in a highly reliable manner. ^{18}F-FP-CMT revealed nearly optimal properties for PET imaging of DAT in rat, about its lack of a lipophilic metabolite, and high pharmacological selectivity for DAT. Its moderate affinity for DAT is sufficient to obtain abundant specific binding in the striatum, but with a rapid attainment of equilibrium, such that recordings as brief as 45 minutes suffice for quantitation of BP_{ND} using the cerebellum as a reference tissue. We consider ^{18}F-FP-CMT to be the preferred radiotracer for imaging the DAT in the rat brain, with potential for application in human PET studies.

DISCLOSURE/CONFLICT OF INTEREST

The authors declare no conflict of interest.

ACKNOWLEDGMENTS

The authors thank Manuel Geisthoff and Adelina Haller (Department of Nuclear Medicine, FAU), Dr D Amato (Department of Psychiatry and Psychotherapy, FAU) and André Aichert (Pattern Recognition Lab, FAU) for expert technical support.

REFERENCES

1 Stehouwer JS, Daniel LM, Chen P, Voll RJ, Williams L, Plott SJ *et al.* Synthesis, fluorine-18 radiolabeling, and biological evaluation of N-((E)-4-fluorobut-2-en-1-yl)-2-β-carbomethoxy-3-β-(4′-halophenyl)nortropanes: candidate radioligands for *in vivo* imaging of the brain dopamine transporter with positron emission tomography. *J Med Chem* 2010; **53**: 5549–5557.
2 Riss PJ, Stockhofe K, Roesch F. Tropane-derived ^{11}C-labelled and ^{18}F-labelled DAT ligands. *J Labelled Compd Rad* 2013; **56**: 149–158.
3 Stehouwer JS. Fluorinated Tropanes. *Curr Top Med Chem* 2013; **13**: 920–935.
4 Ziebell M, Holm-Hansen S, Thomsen G, Wagner A, Jensen P, Pinborg LH *et al.* Serotonin transporters in dopamine transporter imaging: a head-to-head comparison of dopamine transporter SPECT radioligands ^{123}I-FP-CIT and ^{123}I-PE2I. *J Nucl Med* 2010; **51**: 1885–1891.
5 Seibyl JP, Marek K, Sheff K, Zoghbi S, Baldwin RM, Charney DS *et al.* Iodine-123-β-CIT and iodine-123-FPCIT SPECT measurement of dopamine transporters in healthy subjects and Parkinson's patients. *J Nucl Med* 1998; **39**: 1500–1508.
6 Tolosa E, Borght TV, Moreno E. DaTSCAN Clinically Uncertain Parkinsonian Syndromes Study Group. Accuracy of DaTSCAN (^{123}I-Ioflupane) SPECT in diagnosis of patients with clinically uncertain parkinsonism: 2-year follow-up of an open-label study. *Movement Disord* 2007; **22**: 2346–2351.
7 Booij J, Andringa G, Rijks LJ, Vermeulen RJ, De Bruin K, Boer GJ *et al.* [^{123}I]FP-CIT binds to the dopamine transporter as assessed by biodistribution studies in rats and SPECT studies in MPTP-lesioned monkeys. *Synapse* 1997; **27**: 183–190.
8 Fowler JS, Volkow ND, Wang GJ, Gatley SJ, Logan J. [^{11}C]Cocaine: PET studies of cocaine pharmacokinetics, dopamine transporter availability and dopamine transporter occupancy. *Nucl Med Biol* 2001; **28**: 561–572.
9 Volkow ND, Fowler JS, Logan J, Gatley SJ, Dewey SL, Macgregor RR *et al.* Carbon-11-cocaine binding compared at subpharmacological and pharmacological doses—a PET study. *J Nucl Med* 1995; **36**: 1289–1297.
10 Doudet DJ, Rosa-Neto P, Munk OL, Ruth TJ, Evan S, Cumming P. Effect of age on markers for monoaminergic neurons of normal and MPTP-lesioned rhesus monkeys: A multi-tracer PET study. *Neuroimage* 2006; **30**: 26–35.
11 Han DD, Gu HH. Comparison of the monoamine transporters from human and mouse in their sensitivities to psychostimulant drugs. *BMC Pharmacol* 2006; **6**: 6.
12 Shetty HU, Zoghbi SS, Liow JS, Ichise M, Hong J, Musachio JL *et al.* Identification and regional distribution in rat brain of radiometabolites of the dopamine transporter PET radioligand [^{11}C]PE2I. *Eur J Nucl Med Mol Imaging* 2007; **34**: 667–678.
13 Peyronneau MA, Saba W, Dolle F, Goutal S, Coulon C, Bottlaender M *et al.* Difficulties in dopamine transporter radioligand PET analysis: the example of LBT-999 using [^{18}F] and [^{11}C] labelling Part II: metabolism studies. *Nucl Med Biol* 2012; **39**: 347–359.
14 Riss PJ, Debus F, Hummerich R, Schmidt U, Schloss P, Lueddens H *et al. Ex vivo* and *in vivo* evaluation of [^{18}F]PR04.MZ in rodents: a selective dopamine transporter imaging agent. *Chem Med Chem* 2009; **4**: 1480–1487.
15 Zoghbi SS, Shetty HU, Ichise M, Fujita M, Imaizumi M, Liow JS *et al.* PET imaging of the dopamine transporter with ^{18}F-FECNT: A polar radiometabolite confounds brain radioligand measurements. *J Nucl Med* 2006; **47**: 520–527.
16 Ma Y, Dhawan V, Mentis M, Chaly T, Spetsieris PG, Eidelberg D. Parametric mapping of [^{18}F]FPCIT binding in early stage Parkinson's disease: a PET study. *Synapse* 2002; **45**: 125–133.
17 Davis MR, Votaw JR, Bremner JD, Byas-Smith MG, Faber TL, Voll RJ *et al.* Initial human PET imaging studies with the dopamine transporter ligand ^{18}F-FECNT. *J Nucl Med* 2003; **44**: 855–861.
18 Goodman MM, Kilts CD, Keil R, Shi B, Martarello L, Xing DX *et al.* ^{18}F-labeled FECNT: a selective radioligand for PET imaging of brain dopamine transporters. *Nucl Med Biol* 2000; **27**: 1–12.
19 Forsback S, Marjamaki P, Eskola O, Bergman J, Rokka J, Gronroos T *et al.* [^{18}F]CFT synthesis and binding to monoamine transporters in rats. *EJNMMI research* 2012; **2**: 3.
20 Gu XH, Zong R, Kula NS, Baldessarini RJ, Neumeyer JL. Synthesis and biological evaluation of a series of novel N- or O-fluoroalkyl derivatives of tropane: potential positron emission tomography (PET) imaging agents for the dopamine transporter. *Bioorg Med Chem Lett* 2001; **11**: 3049–3053.
21 Chaly T, Matacchieri R, Dahl R, Dhawan V, Eidelberg D. Radiosynthesis of [^{18}F]N-3-fluoropropyl-2-β-carbomethoxy-3-β (4′-methylphenyl) nortropane (FPCMT). *Appl Radiat Isotopes* 1999; **51**: 299–305.
22 Quik M, Sum JD, Whiteaker P, McCallum SE, Marks MJ, Musachio J *et al.* Differential declines in striatal nicotinic receptor subtype function after nigrostriatal damage in mice. *Mol Pharmacol* 2003; **63**: 1169–1179.
23 Gillings NM, Bender D, Falborg L, Marthi K, Munk OL, Cumming P. Kinetics of the metabolism of four PET radioligands in living minipigs. *Nucl Med Biol* 2001; **28**: 97–104.
24 Cumming P, Yokoi F, Chen A, Deep P, Dagher A, Reutens D *et al.* Pharmacokinetics of radiotracers in human plasma during positron emission tomography. *Synapse* 1999; **34**: 124–134.
25 Lammertsma AA, Hume SP. Simplified reference tissue model for PET receptor studies. *Neuroimage* 1996; **4**: 153–158.
26 Isovich E, Mijnster MJ, Flugge G, Fuchs E. Chronic psychosocial stress reduces the density of dopamine transporters. *Eur J Neurosci* 2000; **12**: 1071–1078.
27 Zhou Y, Endres CJ, Brasic JR, Huang SC, Wong DF. Linear regression with spatial constraint to generate parametric images of ligand-receptor dynamic PET studies with a simplified reference tissue model. *Neuroimage* 2003; **18**: 975–989.

28 Logan J, Fowler JS, Volkow ND, Wolf AP, Dewey SL, Schlyer DJ *et al.* Graphical analysis of reversible radioligand binding from time-activity measurements applied to [N-^{11}C-methyl]-(−)-cocaine PET studies in human subjects. *J Cereb Blood Flow Metab* 1990; **10**: 740–747.
29 Logan J, Fowler JS, Volkow ND, Wang GJ, Ding YS, Alexoff DL. Distribution volume ratios without blood sampling from graphical analysis of PET data. *J Cereb Blood Flow Metab* 1996; **16**: 834–840.
30 Sossi V, Dinelle K, Jivan S, Fischer K, Holden JE, Doudet D. *In Vivo* dopamine transporter imaging in a unilateral 6-hydroxydopamine rat model of Parkinson disease using ^{11}C-methylphenidate PET. *J Nucl Med* 2012; **53**: 813–822.
31 Hume SP, Brown DJ, Ashworth S, Hirani E, Luthra SK, Lammertsma AA. *In vivo* saturation kinetics of two dopamine transporter probes measured using a small animal positron emission tomography scanner. *J Neurosci Meth* 1997; **76**: 45–51.
32 Cumming P. Absolute abundances and affinity states of dopamine receptors in mammalian brain: a review. *Synapse* 2011; **65**: 892–909.
33 Guo Q, Brady M, Gunn RN. A biomathematical modeling approach to central nervous system radioligand discovery and development. *J Nucl Med* 2009; **50**: 1715–1723.
34 Fujita M, Shimada S, Fukuchi K, Tohyama M, Nishimura T. Distribution of cocaine recognition sites in rat-brain—in-vitro and ex-vivo autoradiography with [^{125}I]RTI-55. *J Chem Neuroanat* 1994; **7**: 13–23.
35 Liu JY, Zhu L, Plossl K, Lieberman BP, Kung HF. Synthesis and evaluation of novel N-fluoropyridyl derivatives of tropane as potential PET imaging agents for the dopamine transporter. *Bioorg Med Chem Lett* 2011; **21**: 2962–2965.
36 Wuest F, Berndt M, Strobel K, van den Hoff J, Peng X, Neumeyer JL *et al.* Synthesis and radiopharmacological characterization of 2 beta-carbo-2 '-[^{18}F]fluoroethoxy-3 β-(4-bromo-phenyl)tropane ([^{18}F]MCL-322) as a PET radiotracer for imaging the dopamine transporter (DAT). *Bioorg Med Chem* 2007; **15**: 4511–4519.
37 Dollé F, Emond P, Mavel S, Demphel S, Hinnen F, Mincheva Z *et al.* Synthesis, radiosynthesis and *in vivo* preliminary evaluation of [^{11}C]LBT-999, a selective radioligand for the visualisation of the dopamine transporter with PET. *Bioorg Med Chem* 2006; **14**: 1115–1125.
38 Gallezot JD, Weinzimmer D, Nabulsi N, Lin SF, Fowles K, Sandiego C *et al.* Evaluation of [^{11}C]MRB for assessment of occupancy of norepinephrine transporters: Studies with atomoxetine in non-human primates. *Neuroimage* 2011; **56**: 268–279.
39 Strazielle C, Lalonde R, Amdiss F, Botez MI, Hebert C, Reader TA. Distribution of dopamine transporters in basal ganglia of cerebellar ataxic mice by [^{125}I]RTI-121 quantitative autoradiography. *Neurochem Int* 1998; **32**: 61–68.
40 Pedersen K, Simonsen M, Ostergaard SD, Munk OL, Rosa-Neto P, Olsen AK *et al.* Mapping the amphetamine-evoked changes in [^{11}C]raclopride binding in living rat using small animal PET: modulation by MAO-inhibition. *Neuroimage* 2007; **35**: 38–46.
41 Riss PJ, Hooker JM, Alexoff D, Kim SW, Fowler JS, Rosch F. [^{11}C]PR04.MZ, a promising DAT ligand for low concentration imaging: synthesis, efficient ^{11}C-*O*-methylation and initial small animal PET studies. *Bioorg Med Chem Lett* 2009; **19**: 4343–4345.
42 Riss PJ, Hummerich R, Schloss P. Synthesis and monoamine uptake inhibition of conformationally constrained 2 β-carbomethoxy-3 β-phenyl tropanes. *Org Biomol Chem* 2009; **7**: 2688–2698.
43 Meltzer PC, Liang AY, Brownell AL, Elmaleh DR. Madras BK. Substituted 3-phenyltropane analogs of cocaine: synthesis, inhibition of binding at cocaine recognition sites, and positron emission tomography imaging. *J Med Chem* 1993; **36**: 855–862.

Supplementary Information accompanies the paper on the Journal of Cerebral Blood Flow & Metabolism website (http://www.nature.com/jcbfm)